eLIFE elifesciences.org

RESEARCH ARTICLE

Figures and figure supplements

Silent synapses generate sparse and orthogonal action potential firing in adult-born hippocampal granule cells

Liyi Li *et al*

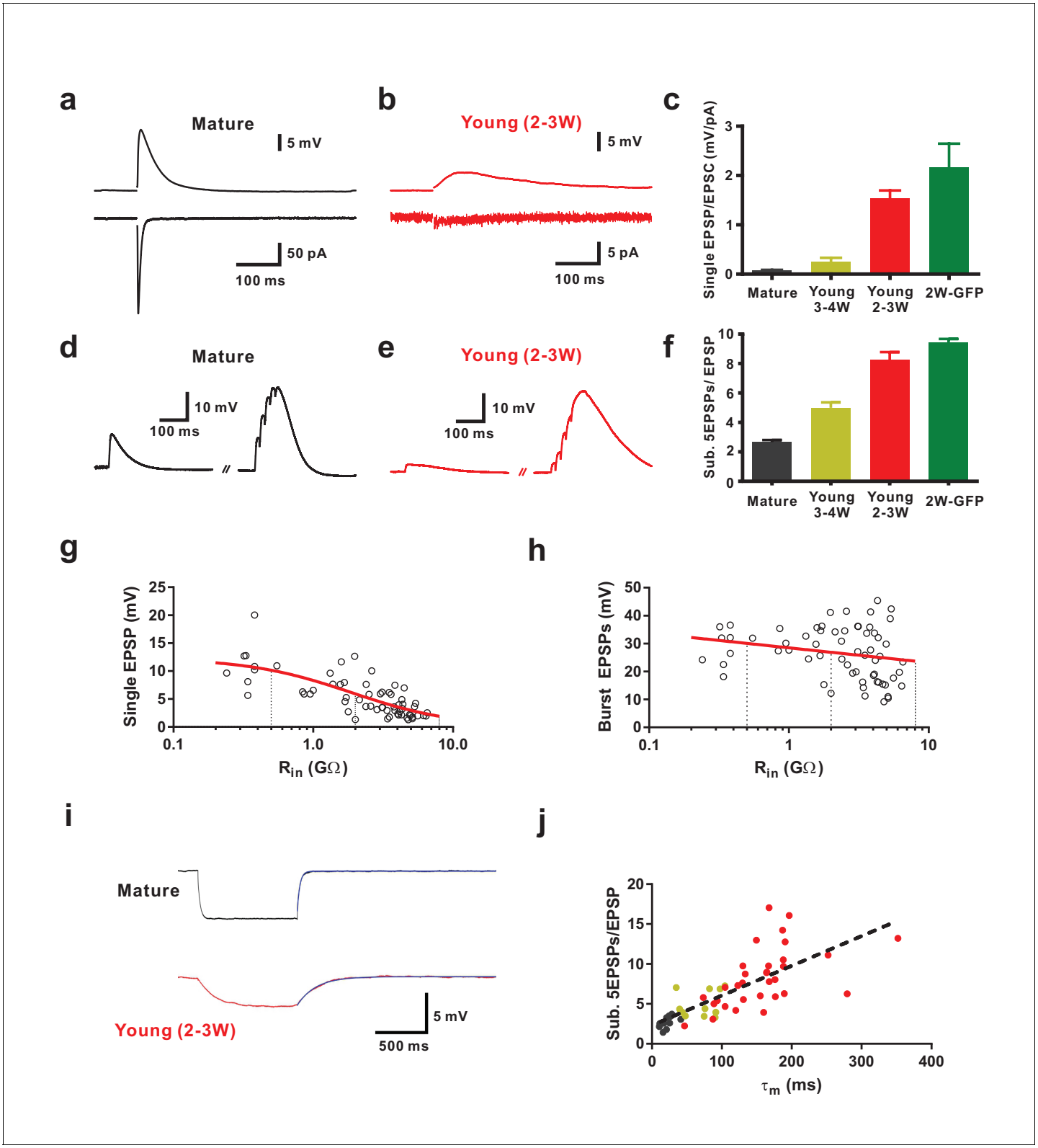

Figure 1. Efficient subthreshold EPSP summation in newborn young granule cells. (**a, b**) Example of synaptic EPSPs (top) and corresponding EPSCs (bottom) in a mature (**a**) and in a DCX-DsRed expressing young granule cell with an estimated age of 2.5 weeks post mitosis (**b**), recorded at resting membrane potential (V_m = −80 mV). Extracellular stimulation intensity was 30 µA with 0.2 ms duration. (**c**) The ratio of synaptic EPSP relative to EPSC amplitude in individual cells is significantly higher in 2 wpi GFP labelled neurons (2W-GFP, $p<0.001$) and 2–3 week old DCX-DsRed labelled neurons

Figure 1 continued on next page

Figure 1 continued

(young 2–3W) relative to mature granule cells ($p<0.0001$, Mann-Whitney). The EPSP/EPSC ratio in 2W-GFP and young 2–3 W cells was not significantly different ($p=0.282$, Mann-Whitney). Bars for mature, 3–4W-DsRed, 2–3W-DsRed and 2W-GFP cells represent data from n = 19, 12, 8 and 6 neurons, respectively. (**d, e**) Subthreshold summation of five EPSPs evoked by brief burst stimuli (5@50 Hz, 20 μA) in a mature (**d**) and a young 2.5 week old GC (**e**). (**f**) The ratio of burst EPSP amplitude to single EPSPs is significantly higher in 2W-GFP ($p<0.0001$, Mann-Whitney) and young 2–3 week old neurons ($p<0.0001$, Mann-Whitney) relative to mature cells. Bars for mature, 3–4W young, 2–3W young and 2W-GFP cells represent data from n = 20, 33, 51 and 11 neurons, respectively. Stimulation intensity: 10–20 μA. (**g, h**) Amplitude of single EPSPs (**g**) and burst EPSPs (h, 5@50 Hz, 20 μA) in young and mature GCs were plotted against R_{in} (n = 63). Single EPSPs (**g**) were fitted with a sigmoidal function, showing a half-maximal amplitude with R_{in} = 1.9 GΩ. Burst EPSPs (**h**) were fitted with linear regression analysis revealing a small but non-significant decrease with R_{in} ($p=0.08$). The vertical dashed lines indicate the R_{in} at 4, 3 and 2 weeks post mitosis. (**i**) Examples of membrane potential hyperpolarization (~5 mV) by small negative current pulses in a mature (top) and young 2.5 week old GC (bottom). The blue curve represents a mono-exponential fit to the repolarization phase for estimation of the membrane time constant (τ_m). (**j**) The ratio of burst EPSP amplitude to single EPSPs significantly correlates with the membrane time constant of young and mature GCs. Dashed line represents a linear regression, showing that the slope is significantly non-zero ($p<0.0001$, n = 55). The dots in black, yellow and red are data points from mature, 3–4 week old DsRed and 2–3 week old DsRed cells, respectively.

DOI: https://doi.org/10.7554/eLife.23612.002

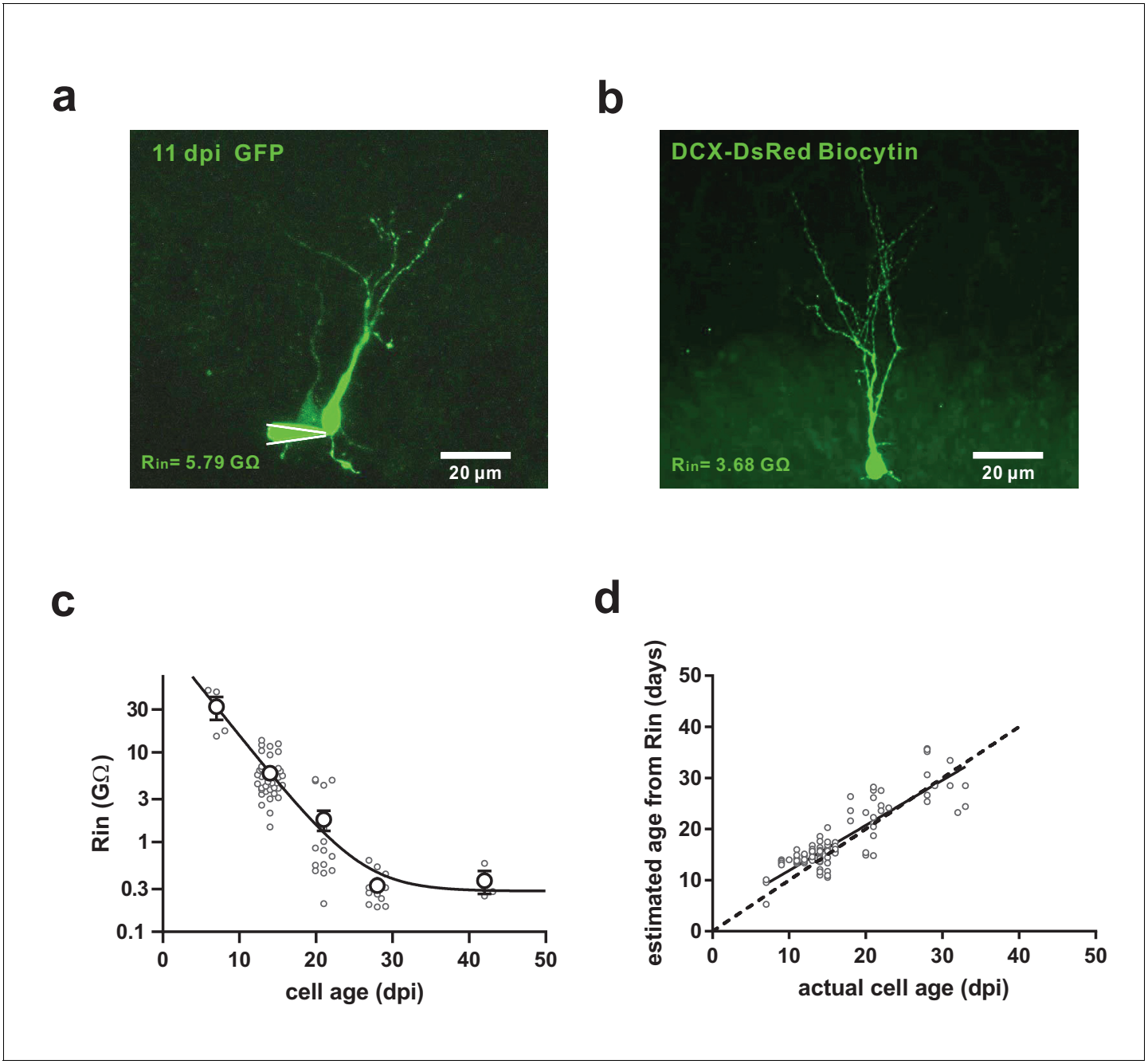

Figure 1—figure supplement 1. Identification of newborn granule cells in the adult mouse hippocampus. (**a**) Confocal image of a retroviral-EGFP labelled young GC at 11 days post injection (11 dpi). White lines represent the recording pipette in cell-attached recording configuration. (**b**) Confocal image of a recorded DCX-DsRed expressing young GC, which was filled with biocytin during whole-cell patch-clamp recording. (**c**) Progressive reduction of input resistance (R_{in}) during the maturation of retroviral-EGFP labelled newborn GCs. Individual cells (small circles) were plotted together with binned data (large circles) at 7 ± 1 dpi (n = 4), 14 ± 1 dpi (n = 41), 21 ± 1 dpi (n = 16), 28 ± 1 dpi (n = 13) and 42 ± 1 dpi (n = 3). The continuous line represents an exponential decay of R_{in} fitted to the binned data (R^2 = 0.75). (**d**) The R_{in} of individual Retrovirus labelled neurons ranging from 7 to 33 dpi was measured and used to calculate an estimated age, using the fitted exponential function shown in c (n = 103). The estimated age was plotted against the actual age measured as time after virus injection. The dashed line represents identity and the continuous line represents a linear fit to the scattered data (slope = 0.88 ± 0.05, R^2 = 0.73, p<0.0001) showing that the estimated age is similar to the actual cell age within the analysed range.
DOI: https://doi.org/10.7554/eLife.23612.003

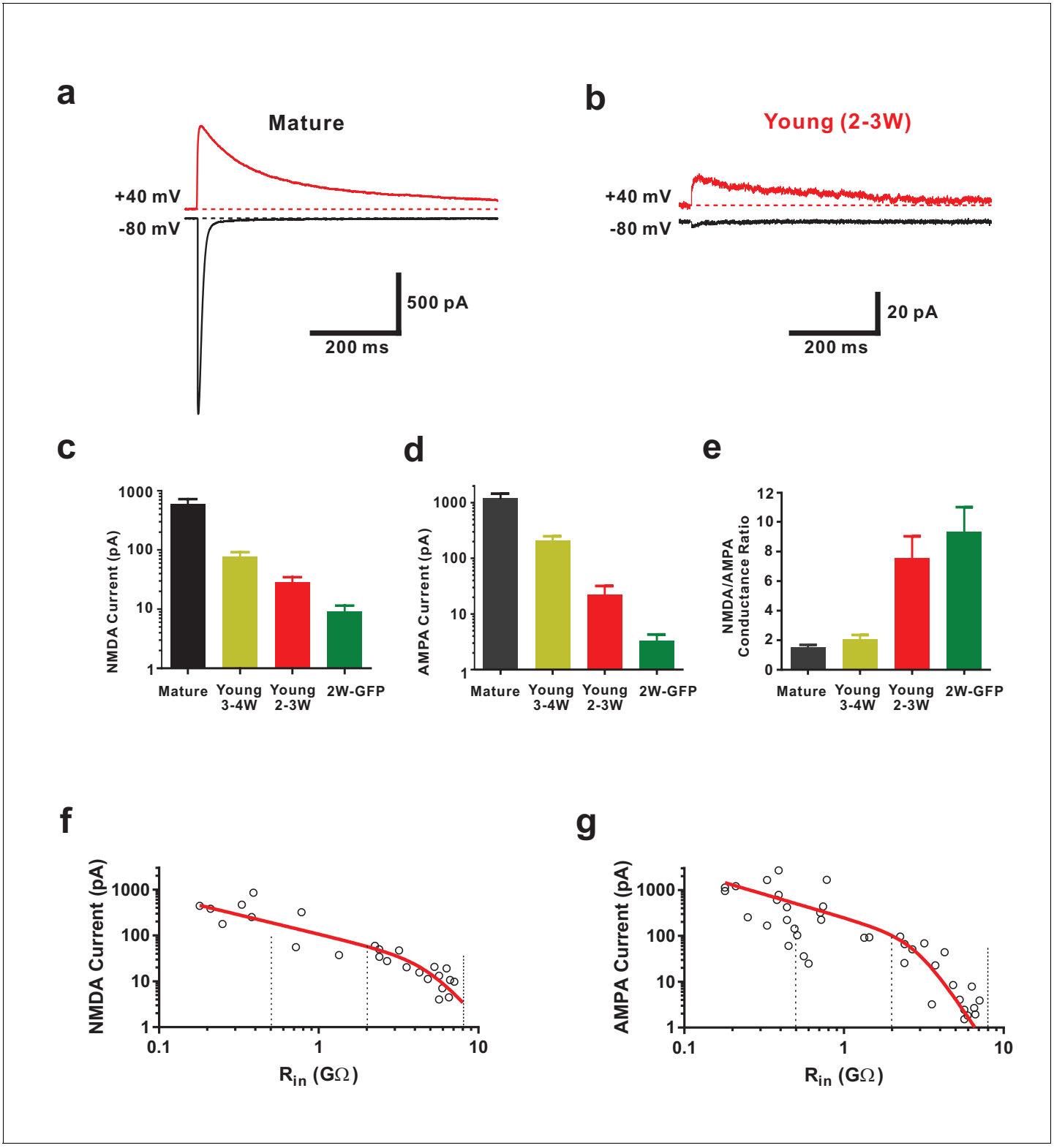

Figure 2. Functional properties of NMDA-receptor mediated EPSCs in young GCs. (**a, b**) Whole-cell voltage-clamp recordings of NMDA-receptor mediated EPSCs in presence of CNQX (top,+40 mV) and of CNQX-sensitive AMPA-mediated EPSCs (bottom, −80 mV) in a mature (**a**) and 2–3 week old DsRed neuron (**b**). (**c**) Bar graph showing the gradual increase of NMDA-receptor mediated EPSCs during the maturation of newborn GCs. All developmental stages are significantly different from each other ($p<0.05$, Mann-Whitney-Test). Bars for mature, 3–4W DsRed, 2–3W DsRed and 2W GFP cells represent data from n = 7, 3, 12 and 6 neurons, respectively. (**d**) Bar graph showing the gradual increase of AMPA-receptor mediated EPSCs. All

Figure 2 continued on next page

Figure 2 continued

developmental stages are significantly different from each other ($p<0.05$, Mann-Whitney-Test). Bars for mature, 3–4W DsRed, 2–3W DsRed and 2W GFP cells represent data from $n = 7$, 3, 12 and 6 neurons, respectively. (**e**) Young 2W-GFP and 2–3 week old DsRed neurons show a significantly higher NMDA- to AMPA-receptor mediated conductance ratio relative to mature GCs ($p<0.05$). Young 2W-GFP and 2–3 week old DsRed neurons are not significantly different form each other ($p=0.43$, Mann-Whitney-Test). Bars for mature, 3–4W DsRed, 2–3W DsRed and 2W GFP cells represent data from $n = 7$, 3, 12 and 6 neurons, respectively. (**f, g**) Amplitude of NMDA currents recorded at +40 mV (f, $n = 28$) and AMPA currents recorded at −80 mV (g, $n = 43$) in young and mature GCs was plotted against log(Rin). The data were fitted with an exponential decay multiplied with a sigmoidal function (see Materials and methods). The vertical dashed lines indicate the R_{in} at 4, 3 and 2 weeks post mitosis.

DOI: https://doi.org/10.7554/eLife.23612.004

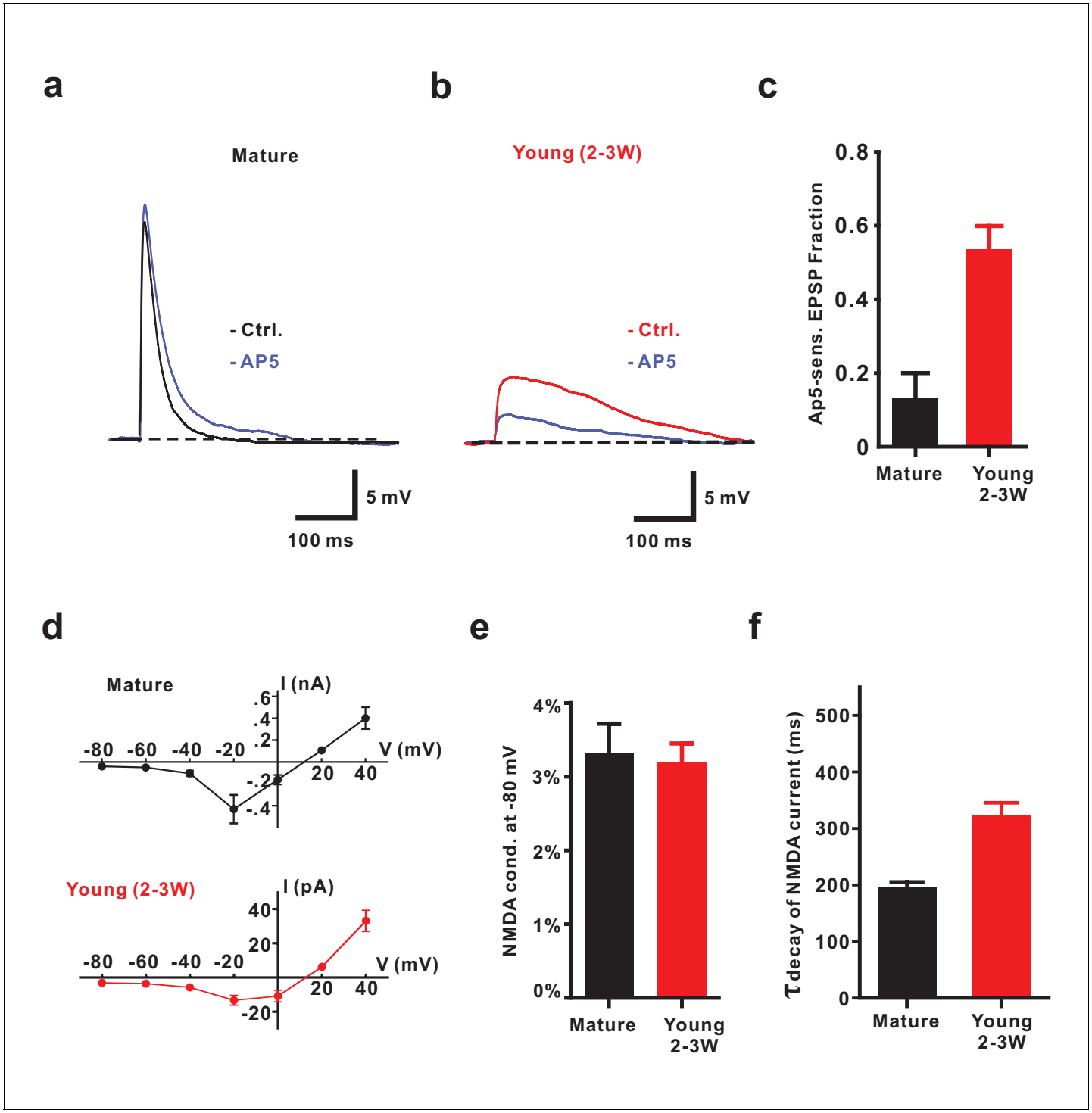

Figure 3. NMDA receptors contribute to EPSPs from resting membrane potential in young GCs. (**a, b**) Application of 50 µM AP5 does not significantly affect EPSP amplitude in mature GCs (**a**) but decreases EPSP amplitude in young neurons (2–3W DsRed, (**b**). (**c**) Bar graph showing a significantly larger contribution of AP5-sensitive NMDA receptors to the EPSP in 2–3 week old DsRed neurons than in mature GCs ($p<0.01$, Mann-Whitney-Test). In contrast to the mild effect of AP5 in mature GCs ($p=0.31$, Wilcoxon Matched Pairs Test, $n = 5$), AP5 application markedly decreased the EPSP amplitude in young GCs ($p<0.01$, Wilcoxon Matched Pairs Test, $n = 9$). (**d**) I-V relationship of synaptic NMDA-receptor mediated currents in mature ($n = 4$, top) and young GCs ($n = 7$, bottom). NMDA receptors in both groups elicited maximal inward currents at −20 mV. (**e**) The ratio of the NMDAR-mediated conductance at −80 mV relative to the conductance at +40 mV was not significantly different between mature ($n = 4$) and young GCs ($n = 6$, $p=0.91$, Mann-Whitney). (**f**) NMDA-receptor mediated EPSCs (recorded at +40 mV) decay significantly slower in young ($n = 11$) than in mature GCs ($n = 7$, $p<0.001$, Mann Whitney).

DOI: https://doi.org/10.7554/eLife.23612.005

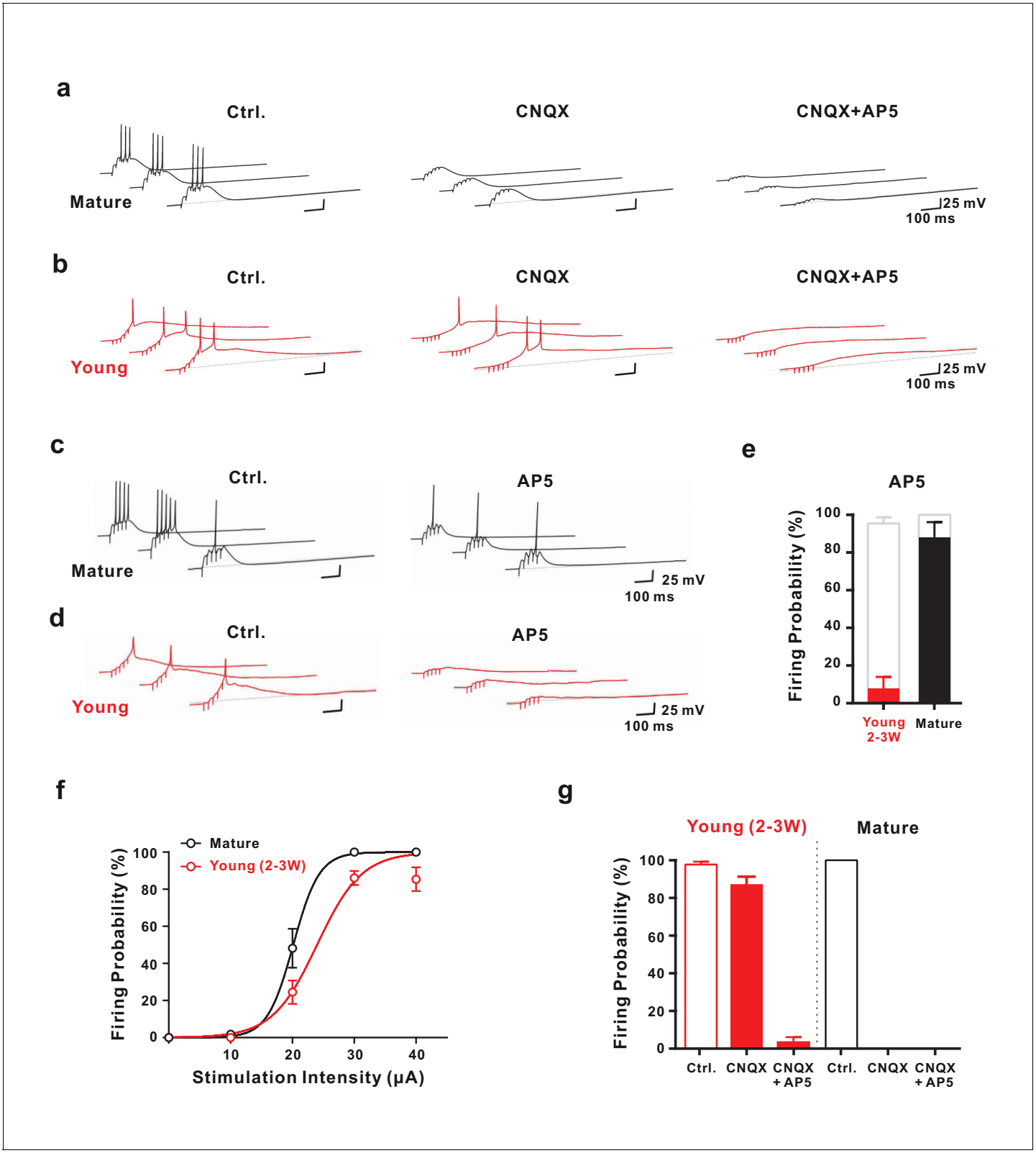

Figure 4. Synaptic NMDA-receptor dependent spiking in young GCs. (**a**,**b**) Synaptically evoked APs in mature GCs (**a**) were blocked by CNQX. By contrast in young GCs (**b**), firing was insensitive to CNQX, while it was fully blocked by AP5 (30 μA). (**c**,**d**) Conversely, in AP5 alone firing was still possible in mature neurons (**c**), but was largely blocked in young GCs (**d**). (**e**) The bar graph summarizes the strong reduction in AP success rate per burst in young cells (7.7 ± 6.2% versus 95.4 ± 3.3% in control, *n* = 13), as well as the small effect in mature GCs (88.0 ± 8.0% versus 100% in control,

Figure 4 continued on next page

Figure 4 continued

n = 5). (**f**) The probability to fire one or more spikes per burst was plotted against stimulation intensity, showing that 2–3 week old DsRed neurons (*n* = 38) reach AP threshold as efficiently as mature GCs (*n* = 22) during burst stimulation. The data were fitted with a sigmoidal function (black and red curves), with half-maximal firing rate at a stimulation intensity of 20.2 µA and 23.6 µA in mature and 2–3 week-old neurons, respectively. (**g**) Bar graphs showing firing probability of the young (red) and mature GCs (black) under pharmacological conditions described in (**a**) and (**b**). Unlike the dominant effect of CNQX on firing in mature GCs (control vs. CNQX: from 100% to 0, *n* = 5), it had only minor effects in young GCs (control vs. CNQX: from 98% to 87%, $p<0.05$, Wilcoxon Matched Pairs Test, *n* = 17). Additional AP5 application effectively eliminated the firing in young GCs. The red bars represent data from *n* = 5 two-week-old GFP and *n* = 12 DCX-DsRed 2–3 week old cells.

DOI: https://doi.org/10.7554/eLife.23612.006

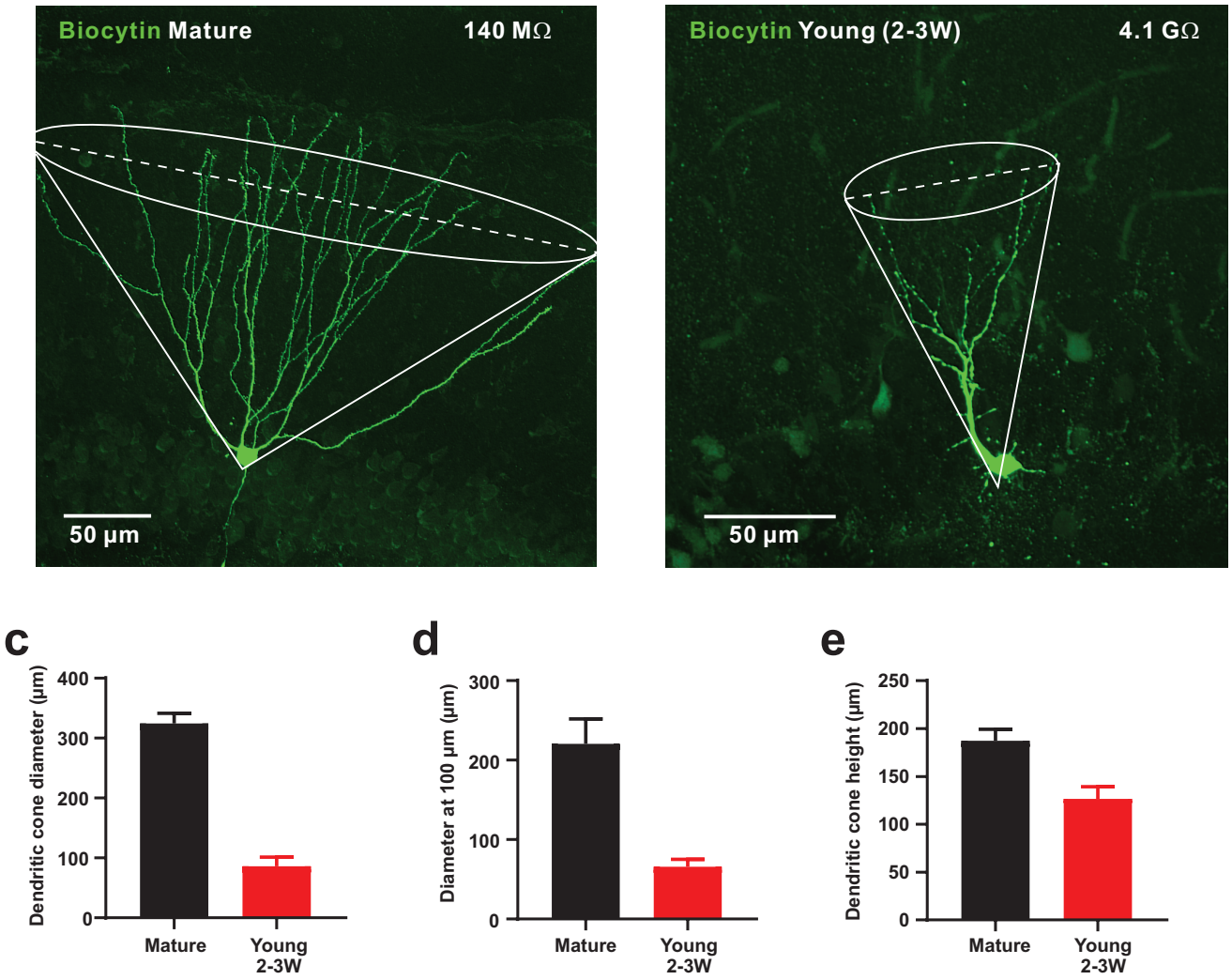

Figure 5. Small diameter of dendritic cones in young GCs. (**a, b**) Morphology of biocytin-filled mature (**a**) and young (**b**) granule cells. The somata are located at the outer and inner border of the granule cell layer, respectively. The cone overlay indicates the geometrical parameters measured, including cone diameter shown as dashed line. (**c–e**). Small diameter of dendritic cone (**c**) in young GCs (n = 8) compared to mature neurons measured at the base. Similarly, the cone diameter was measured at a distance of 100 µm from the soma (**d**). Additionally, the height of the cone is smaller in young versus mature GCs (**e**).

DOI: https://doi.org/10.7554/eLife.23612.007

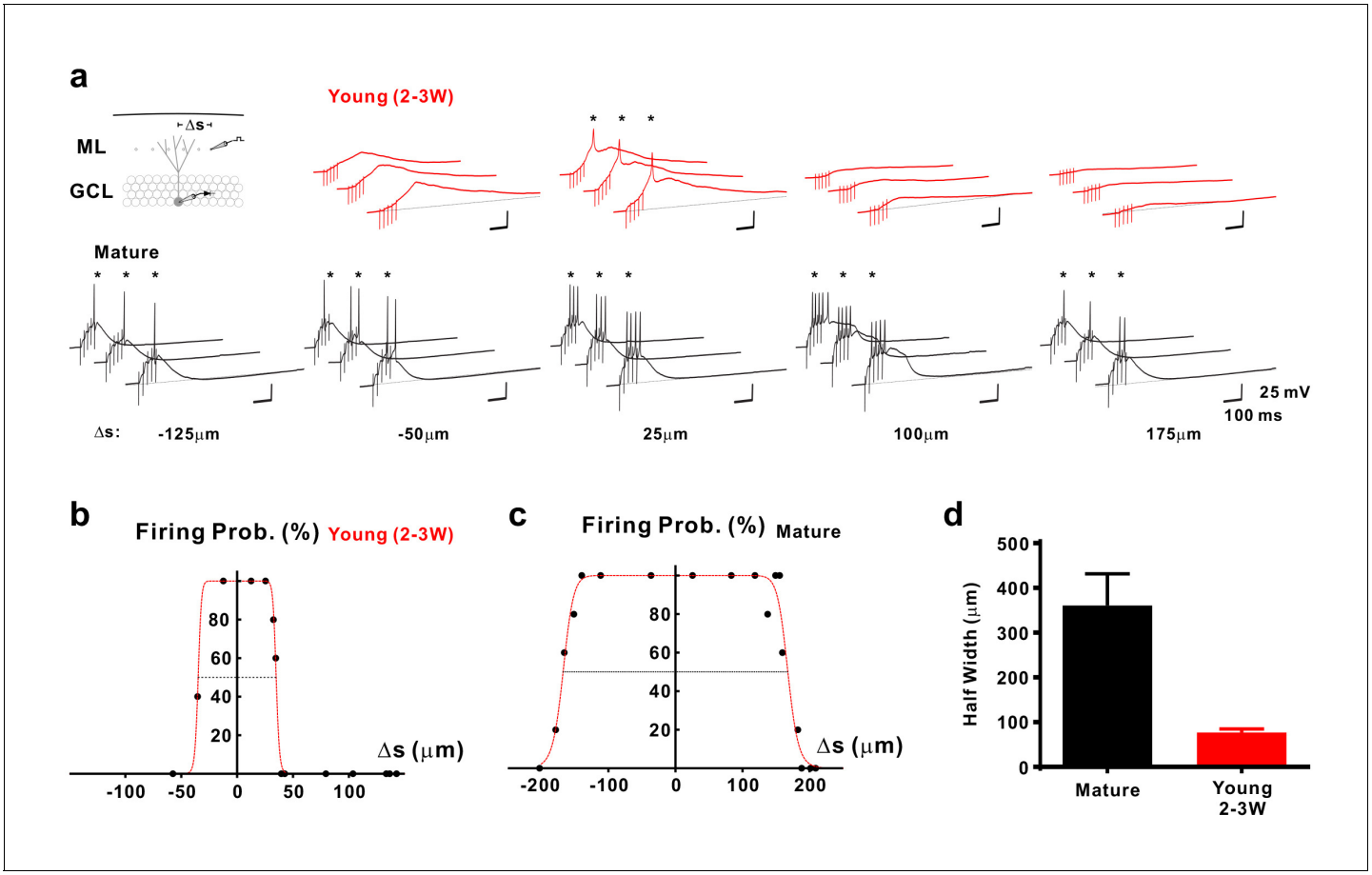

Figure 6. Selective sampling of glutamatergic presynaptic input space in young GCs. (**a**) Synaptically evoked spiking in a 2–3 week old neuron (top) and a mature GC (bottom) with extracellular stimulation at different locations. The stimulation electrode was tangentially shifted in the middle part of the molecular layer (ML) with constant distance of ~100 μm from the granule cell layer (GCL). The schematic diagram of the experimental configuration (top) shows the recorded cell (grey) and the stimulation positions (dots in the ML). *Δ*s represents the distance from the stimulation position to the centre of the spatial range where stimulation generates 100% firing probability. APs are highlighted with stars (*). (**b**,**c**) The firing probability of the young (**b**) and mature cell (**c**) in (**a**) top and bottom, respectively, was plotted against location *Δ*s of the stimulation electrode and fitted with a bell-shaped function (see Materials and methods for details). (**d**) Bar graph showing the mean diameter (half-width) of the dendritic 'firing fields' where APs are generated with more than 50% probability in mature (n = 11) and young (n = 15) GCs. The half-width in young GCs is significantly more narrow than in mature GCs ($p<0.0001$, Mann Whitney).

DOI: https://doi.org/10.7554/eLife.23612.008

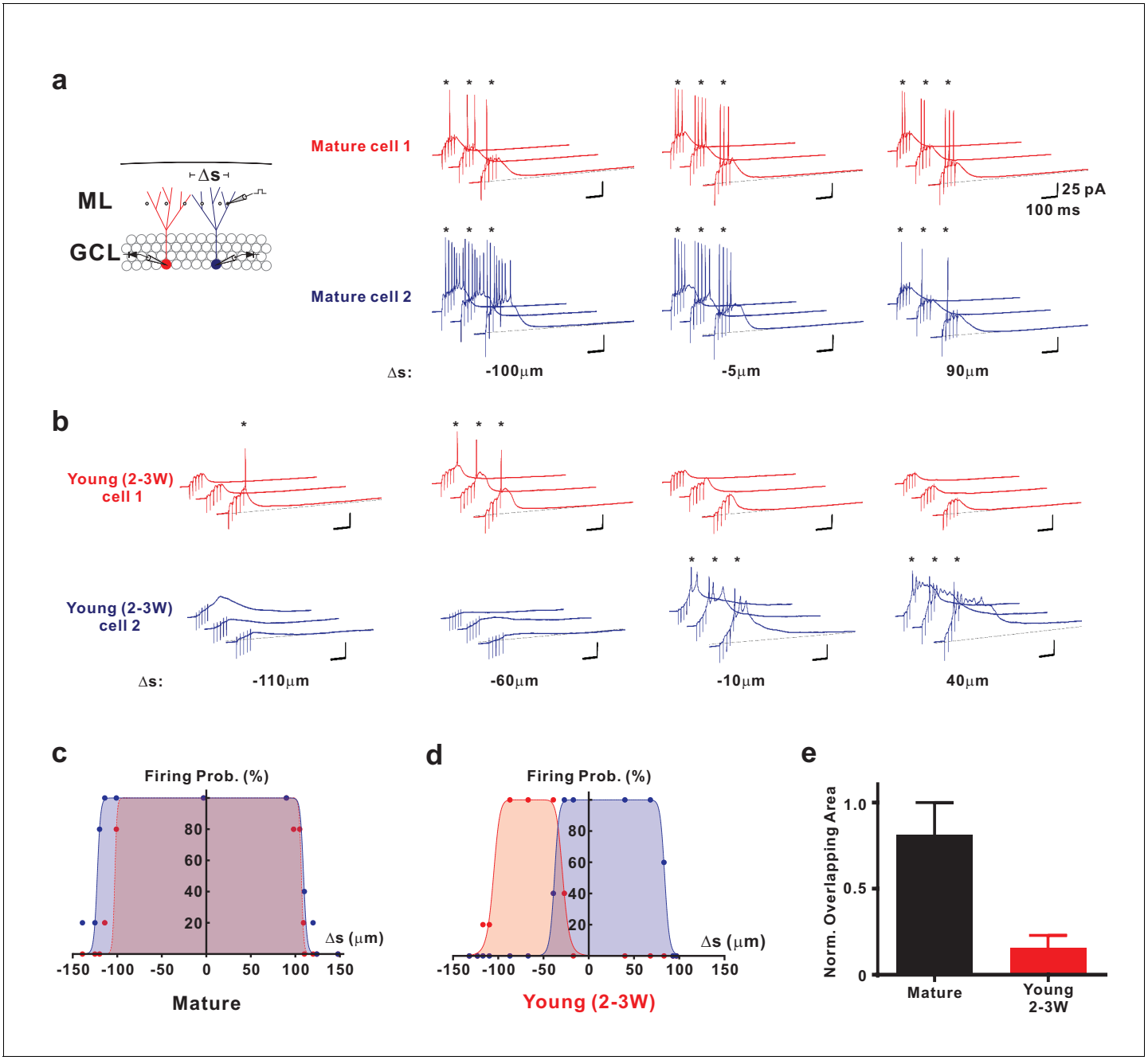

Figure 7. Distinct activation of different young neurons by different afferent fibre subpopulations. (**a**) Synaptically evoked spiking in two simultaneously recorded mature GCs. The stimulation electrode was positioned at different locations Δs along a track parallel to the granule cell layer as indicated. The schematic diagram of the experimental configuration (left) shows the two recorded cells (red and blue) and the stimulation positions (dots in the ML). Δs represents the distance from the stimulation position to the mid-line between the two cells. (**b**) Synaptically evoked spiking in two simultaneously recorded young GCs 2–3 weeks post mitosis at various stimulation positions in the ML. Please note, that the locations to evoke successful firing in two young neurons do not overlap. (**c, d**) The firing probability of the two simultaneously recorded mature (**c**) and young neurons (**d**) shown in a and b, respectively, was plotted against the location Δs of the stimulation electrode. The data were fitted with a bell-shaped function (see Materials and methods for details). Note the small overlap of the area under the curves generated from the young cells (**d**). (**e**) Bar graph showing the normalized overlap of the area under the curve in pairs of mature (n = 8) and young neurons (n = 10, $p<0.001$, Mann Whitney).

DOI: https://doi.org/10.7554/eLife.23612.009

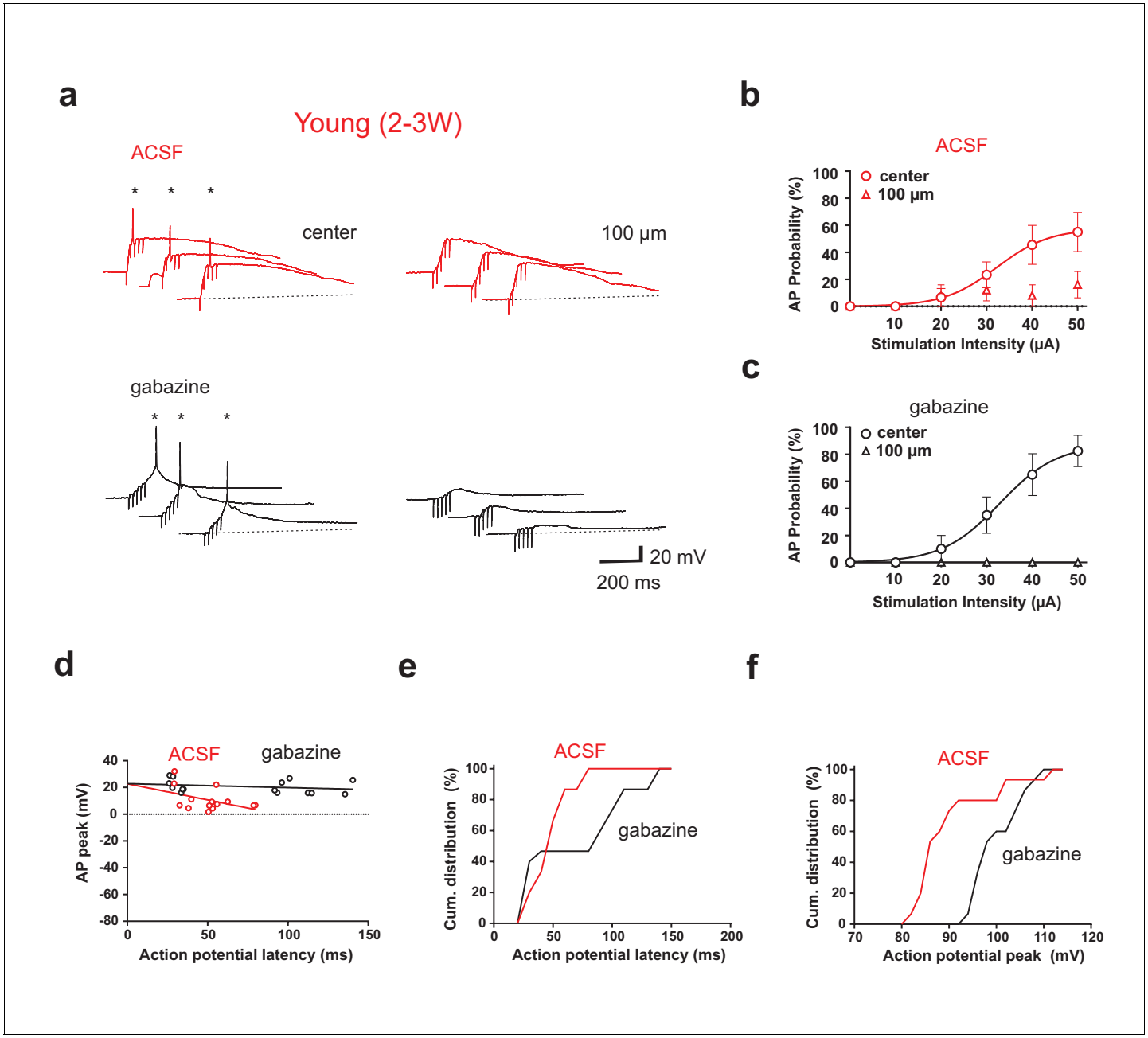

Figure 8. GABAergic synaptic transmission improves temporal precision of young GC firing. (**a**) In ACSF, brief burst stimulation (5@50 Hz) evoked APs in a young GC with the stimulation electrode located in the ML at the center of the dendritic firing field (upper left) but not when the electrode was tangentially shifted by 100 µm (upper right). Similar results were obtained in the presence of gabazine to block GABAergic transmission (lower traces, 50 µA). (**b**) Action potentials were evoked at different stimulation intensities in $n = 6$ out of 9 young cells with center stimulation (circles) but not with a tangentially shifted electrode (triangles). (**c**) Similarly, in the presence of gabazine AP firing in young neurons was restricted to center stimulation ($n = 9$). (**d**) The peak amplitude of the APs from experiments in (**b, c**) was plotted versus AP latency relative to stimulus onset and fitted by linear regression, indicating that AP latencies are shorter in ACSF (50 µA). The slope of the regression line was −24 ± 13 mV/100 ms in ACSF versus −3 ± 3 mV/100 ms in gabazine. (**e, f**) Cumulative distribution of AP latency (**e**) and peak amplitude (**f**) showing that the latency is significantly shorter ($p<0.028$, Kolmogorov-Smirnov) and the peak amplitude is significantly smaller ($p<0.0001$, Kolmogorov-Smirnov) in ACSF.

DOI: https://doi.org/10.7554/eLife.23612.010

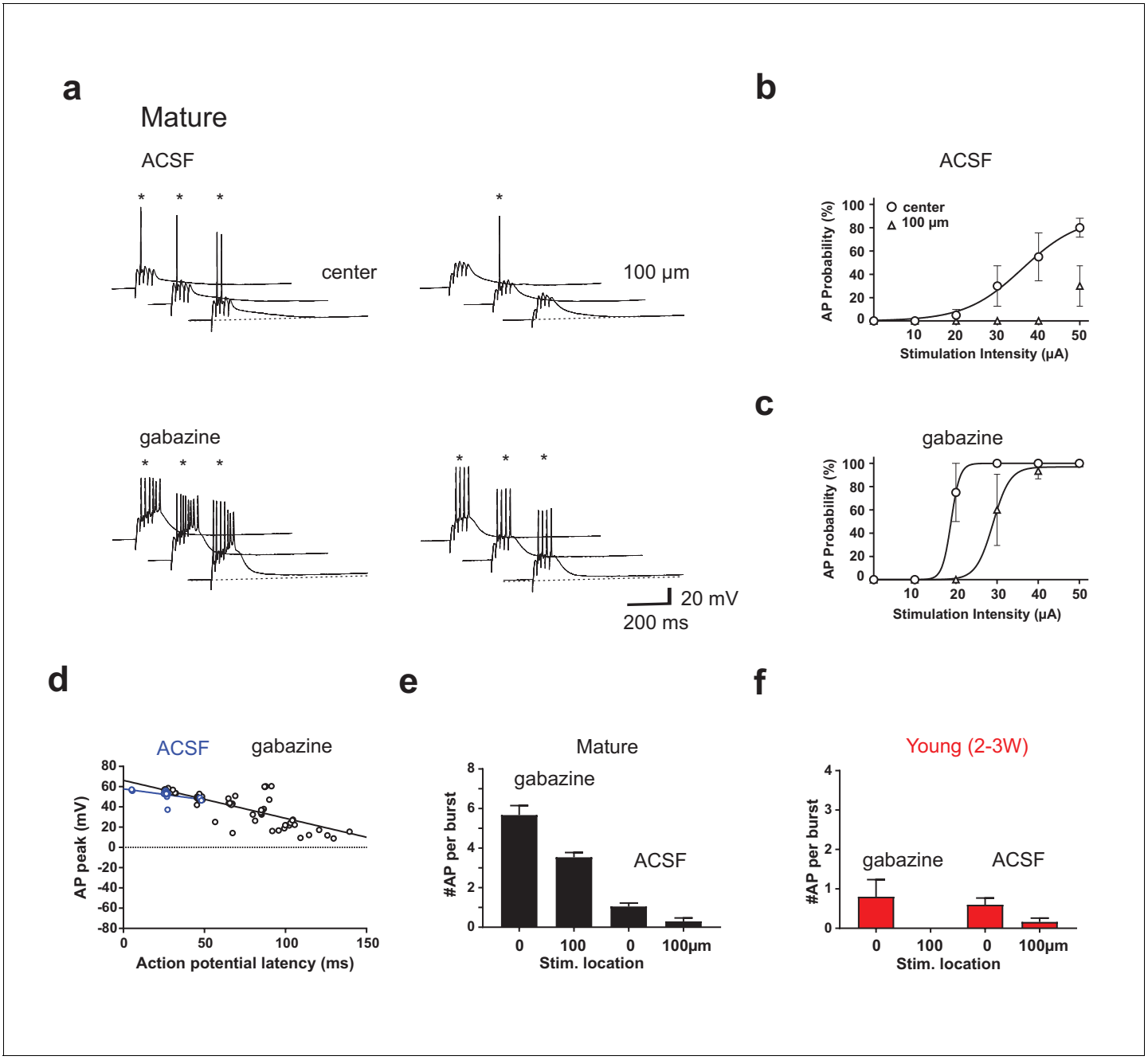

Figure 8—figure supplement 1. GABAergic interneurons strongly decrease burst-evoked AP firing in mature GCs. (**a**) In ACSF, brief burst stimulation (5@50 Hz) reliably evoked APs in a mature GC with the stimulation electrode located in the ML at the center of the dendritic firing field (upper left), but not when the electrode was tangentially shifted by 100 µm (upper right). By contrast, in the presence of gabazine burst evoked firing strongly increased in the center as well as at the 100 µm position (lower right). (**b**) In ACSF action potentials were evoked at different stimulation intensities in *n* = 4 of 6 mature cells with center stimulation (circles), but much less after tangentially shifting the electrode (triangles). (**c**) After gabazine application the mature GCs reliably fired APs in center as wells as after tangential shift of the stimulation electrode (*n* = 4). (**d**) The peak amplitude of the APs from experiments in (**b, c**) was plotted versus AP latency relative to stimulus onset and fitted by linear regression (50 µA). (**e,f**) Bar graphs showing the average number of spikes per burst in mature (e, *n* = 4) and young neurons (f, *n* = 6) with center stimulation (0 µm) or lateral stimulation (100 µm) in ACSF and in gabazine.

DOI: https://doi.org/10.7554/eLife.23612.011